Proceedings of the 26th International Conference on Offshore Mechanics and Arctic Engineering
OMAE2007
June 10-15, 2007, San Diego, California, USA

OMAE2007-29172

DEEP WATER RISER COLLISION AVOIDANCE BY TOP TENSION CONTROL

Anne M. Rustad *
Center for Ships and Ocean Structures (CeSOS)
Norwegian University of
Science and Technology (NTNU)
N-7491 Trondheim, Norway
Email: annemar@ntnu.no

Carl M. Larsen
Asgeir J. Sørensen
Department of Marine Technology
Center for Ships and Ocean Structures (CeSOS)
Norwegian University of
Science and Technology (NTNU)
N-7491 Trondheim, Norway
Email: carl.m.larsen, asgeir.sorensen@ntnu.no

ABSTRACT

For tensioned riser arrays in deep waters interference between individual risers in strong ocean current is a key design and operational concern. The lateral deflections are likely to be large, and the risers may experience collision with fatigue or surface damage as a consequence. In this paper a system consisting of a tension leg platform (TLP), a pair of risers, environmental forces and hydrodynamic interaction is presented. The control system is described, and a set of control objectives with corresponding control strategies are suggested. The collision avoidance effects of the different control objectives are shown through simulations.

INTRODUCTION

The depletion of oil and gas in shallow waters has moved the industry to deeper waters where new technical challenges arise and new solutions need to be found. Riser technology is an important issue both when considering field development costs and technological feasibility. Interaction and collision between adjacent top tensioned risers in an array is an issue of considerable concern, and has been studied by several scientists the last decade, see for instance Huse [1], Wu *et al.* [2], Herfjord *et al.* [3] and Kalleklev *et al.* [4]. The risk of collision increase with increasing water depth, as the static deflection due to the uniform current drag is proportional to the square of the length, see Huse [1]. In deep water this means that even a relatively small difference in the static deflection may lead to mechanical contact. In addition, hydrodynamic interaction forces may cause low frequency riser oscillations of very irregular behavior and large amplitudes. Such motions have been observed and described by Huse [5] and Wu *et al.* [2].

Collision may lead to dents in the riser pipe and damage in the coating, with fatigue and corrosion as possible consequences. Even a single collision incident may be damaging, if the collision takes place with sufficiently high impact. The current design practice does not allow collision under normal or extreme conditions, see DNV [6]. Ensuring no interference between risers by increasing the riser spacing may result in significant cost penalties due to influence on global platform parameters, like deck space and load carrying capacity. Control of top tension is another parameter reducing the number of collisions. However, increasing the top tension to a high and constant level is also expensive and will increase the wear and tear on the cylinders in the heave compensation system.

We will in this paper investigate the possibility to reduce the riser interference by use of automatic control of the riser top tension. A control strategy based on equal payout for all risers in an array was proposed by Huse and Kleiven [7]. Results from the model tests were that the equal payout by connecting all the risers to one common frame at the top end gave a significant reduction of the probability of collision in steady current. This paper is motivated by the work of Huse and Kleiven [7],

*Address all correspondence to this author.

but instead of keeping the risers fixed to a plate, the top tension of each riser is controlled individually using the payout of the heave compensator as the measured input as proposed by Rustad *et al.* [8]. The top tensioned riser control system includes both the physical structure with identification of the limitations and the software implementation with controller objective and algorithm. This paper is an extension of the work presented in Rustad *et al.* [8], including a new controller accounting for the variations in the riser's axial strain. This effect is in particular important for deep water installations.

The paper is organized as follows: Section 2 explains the modelling of the system, including the hydrodynamics of the current field. The controller design is presented in Section 3, while simulations and results are found in Section 4. Section 5 gives the concluding remarks.

MODELLING

The modelled system in this paper consists of two risers connected to a TLP through the top nodes, forcing the top nodes to follow the prescribed motion from the TLP in the horizontal direction. The top nodes are free in the vertical direction, only affected by the top tension acting as a vertical force. In addition the risers are exposed to current forces that are found by considering the hydrodynamic interactions between the risers. The current is modelled as an in-plane profile with varying velocity through the water column. The TLP is exposed to surface current, wind and waves. This section includes the hydrodynamic interaction between the risers, and a brief description of the model. For a more extensive description of the modelling and verification, see Rustad *et al.* [9].

Hydrodynamic Interaction

Kalleklev *et al.* [4] have shown that interaction between two neighboring risers will not have any hydrodynamic influence on the upstream riser (R1) beyond a certain point. Hence, R1 can be treated as an isolated riser. The attention will therefore be given to the hydrodynamic influence on the downstream riser (R2).

R2 experiences reduced mean drag force due to the shielding effect, depending on the location in the wake. A semi-empirical static wake formulation to account for the hydrodynamic interaction between the individual risers in steady current was proposed by Huse [1]. The reduced velocity field in the wake of the upstream cylinder, see Fig. 1, is given by

$$V_r(x,y) = k_2 V_c \sqrt{\frac{C_D D_e}{x_s}} e^{-0.693\left(\frac{y}{b}\right)^2}, \tag{1}$$

where V_c is the incoming current velocity on R1, C_D is the drag coefficient, D_e is the diameter of the upstream riser, and y is the distance away from the centerline of the incoming velocity profile. x_s and b are defined as

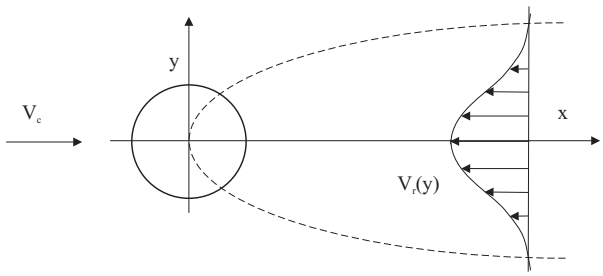

Figure 1. The decrease in the in-line water particle velocity in the wake region, from Huse [1].

$$x_s = x + \frac{4D_e}{C_D}, \quad b = k_1\sqrt{C_D D_e x_s}, \tag{2}$$

where $k_1 = 0.25$ and $k_2 = 1.0$ for a smooth cylinder. x is the distance behind the upstream riser R1, and x_s is the distance between the downstream riser R2 and a virtual wake source upstream of R1. Hence, the mean inflow on the downstream riser is given by

$$V_{mean} = V_c - V_r. \tag{3}$$

It is assumed that the mechanical contact occurs when the distance between the riser centers is equal to one riser diameter (1D). The parametric wake model is only applicable for the far wake region larger than two diameters (2D) behind R1. The behavior of the flow in the near region is not adequately described as this is a highly nonlinear phenomenon, where R2 might experience negative drag forces, see Kavanagh *et al.* [10]. The center-to-center distance should therefore preferably be kept larger than 2D.

Riser Mechanics

Interaction between two cylinders are often classified into two categories according to the space between them; the *proximity interference* when the two cylinders are close to each other, and *wake interference* when one cylinder is in the wake of an upstream cylinder. It is also found that the in-line motion are much larger than the transverse motion. Hence, in this paper we will focus on two risers in a tandem arrangement, were the centers of the two cylinders are aligned parallel to the free stream. A two dimensional model will capture the most important dynamics of the riser array system.

The stiffness matrix in the finite element (FE) model have an elastic and a geometric component. The elastic stiffness matrix accounts for the axial and bending stiffness that is present in any

beam, while the geometric stiffness matrix will take into account the global geometry and the stiffening effect from the tension. For increasing depth, the riser will behave more and more like a cable, making the geometric stiffness more important than the elastic stiffness. At larger water depth, a simplification of the riser model can be made by neglecting the bending stiffness and assuming free rotations in the ends. In cases where the global geometry is of major importance this will only introduce a small error. The dynamic equation of motion is written

$$\mathbf{M}(\mathbf{r})\ddot{\mathbf{r}} + \mathbf{C}(\mathbf{r})\dot{\mathbf{r}} + \mathbf{K}(\mathbf{r})\mathbf{r} = \mathbf{f}_{top} + \mathbf{f}_{cur} - \mathbf{f}_{TLP}, \qquad (4)$$

where $\mathbf{r}$ is the riser position vector. The mass, $\mathbf{M}$, and stiffness, $\mathbf{K}$, matrices are found from FEM analysis, and the damping matrix by using a Rayleigh damping model. The external forces include the forces applied to the top tension, $\mathbf{f}_{top}$, the drag forces from current and riser motion $\mathbf{f}_{cur}$ found from Morison's equation, and terms originating from know TLP motions, $\mathbf{f}_{TLP}$. In Eq. (4) the fixed and prescribed degrees of freedom are removed from the equation, and the influence from specified dofs is included on the right hand side as a force acting on the system. The present model has node 1 with z equal to zero at the sea bed, which leads to

$$\mathbf{r} = \begin{bmatrix} x_2 \; z_2 \; \cdots \; x_i \; z_i \; \cdots \; x_n \; z_n \; z_{n+1} \end{bmatrix}^T. \qquad (5)$$

Current Profiles

The TLP/riser system is, as a base case, simulated at 1200m water depth. Current profiles for three different geographic areas are chosen to compare the behavior of the risers. Amongst these are design profiles representing the Ormen Lange field in the North Sea, Hydro and Aker Maritime [11], loop eddies in the Golf of Mexico (GoM), Nowlin Jr. *et al.* [12] and a bidirectional shear current, see Fig. 2. The Ormen Lange current profile is close to a shelf edge. The velocities are strong all the way down to the sea bed, but even stronger close to the sea surface due to wind generated current. The data from the Ormen Lange field is extended from 850m to 1200m water depth and the current between these depths are considered constant at 0.5m/s. In the current profiles representing the GoM a loop eddy is seen to reduce the current at 200-400m water depth, whereas the velocity increases again for even larger water depths. The bidirectional shear current is due to typically residual warm flow northeastward usually in the upper layer, and a southwestern cold flow in the lower layer. In addition to the residual flow there are tidal current, that do not vary with depth, see Jeans *et al.* [13].

Model Verification

RIFLEX [14] is a commercial FEM program for static and dynamic analysis of slender marine structures. For the purpose

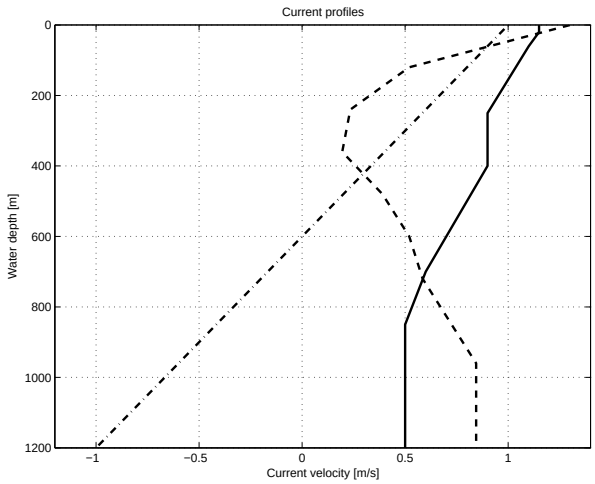

Figure 2. Simulated current profiles from the Ormen Lange field (–), Golf of Mexico (- -) and a bidirectional shear current (-.).

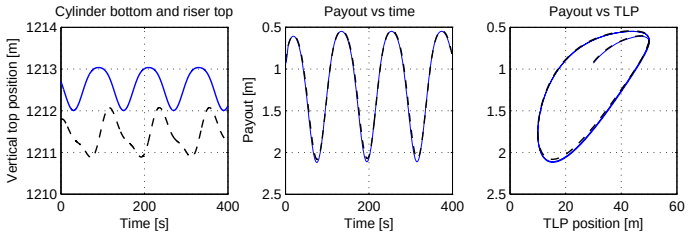

Figure 3. From left: a) Vertical top position of the cylinder bottom (–) and the riser top (- -), b) the distance between them; payout for RIFLEX(–) and Simulink (- -), and c) payout vs TLP position, RIFLEX(–) and Simulink(- -).

of control system design, the present numerical procedure and software code have been implemented in Matlab/Simulink. The model is verified with RIFLEX. The numeric integration used is the Newmark-β method with constant acceleration in each time step. The algorithm implemented is equivalent to what is found in RIFLEX. In order to limit the computation time, it is of interest to minimize the number of finite elements applied in the riser model, while still maintaining a sufficient level of accuracy. The riser model in RIFLEX consists of 404 elements, each 3m long, giving a total length of 1212m. The Matlab/Simulink model consists of 10 elements, each of length 121.2m. The model is tested for both quasi-static and dynamic changes in both the TLP motion and the top tension variation. The change in top position and payout for a dynamically moving TLP with sinusoidal motion of 40m peak-to-peak amplitude, 30m static offset and periods of 120s, is seen in Fig. 3. As seen in Fig. 3b) and c) it is a good correspondence between the model in Matlab/Simulnk and RIFLEX.

CONTROLLER SYSTEM DESIGN

Sørensen [15] addressed the typical various levels of control used in marine control systems. The real time control structure is suggested being divided into *low level actuator control*, *high level plant control* and *local optimization*. The first of these is the actual physical hardware system with local controllers, here represented by the *heave compensator* or *riser tensioner system*. The latter two are parts of the control system architecture or software solution. The local optimizer consists of a guidance block which decides the reference coordinates for the vertical top position for all risers. For each riser there is a reference block, calculating the feasible reference trajectory. The plant controller for each riser then calculates the necessary tension that the corresponding actuator will force on its riser system.

Actuator and Constraints

The riser tensioner system or heave compensator can be implemented as a hydraulic cylinder with a piston. Today this setup strive to keep the tension close to constant. This is obtained by using a compressed air volume as a soft spring in the hydraulic system. Hence, no active control is needed. Designing the heave compensator such that the payout is controlled, will still give the same physical constraints. These could be divided into two groups; (1) constraints due to stroke and (2) constraints due to tension. The stroke parameters are based on the definitions by Larsen [16], slightly modified, and illustrated in Fig. 4. The *initial position* refers to a riser and platform condition without offset or environmental forces, and a desired level of top tension. The *static position* is given by the defined environmental and operational conditions for the given pretension. *Payout* is the distance between the bottom of the cylinder and the top of the riser, positive downwards. The *stroke variation* is the maximum length variation the tensioner system can provide. The *dynamic stroke* is the length variation needed to tension the riser in a particular condition. The dynamic stroke must compensate for the relative motion between the platform and the riser subject to all environmental conditions.

In addition to the boundaries given by the limitations for payout and stroke, the top tension forced on the riser is physically constrained with upper and lower boundaries. If the tension is too low, i.e. less than the effective weight of the riser, the riser will experience buckling. Hence, the lower limit for tension should be the effective weight with a safety margin. The upper tension limit is restricted by the yield stress for the riser material and chosen such that the stress is less than 40% of the yield stress for steel. A given tensioning system will also have limitations regarding maximum tension due to limitations of the pressure in the hydraulic system.

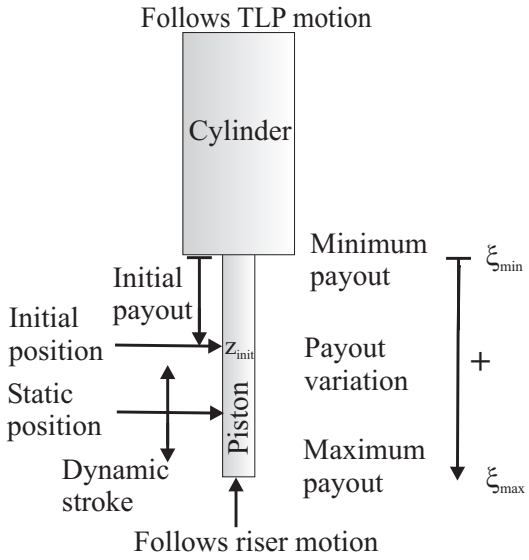

Figure 4. Stroke parameters of one individual cylinder.

Measurements

The non-compensated initial position, z_0, is defined with the design tension and no environmental forces or offsets, and it will be equal for risers with the same physical properties. When the TLP is in an offset position, the setdown of the initial position can be found from the tendon geometry, such that the initial position compensated for setdown, Δs_T is found from

$$z_{init}(t) = z_0 - \Delta s_T(t). \tag{6}$$

The measured parameter used in the control loop is the payout for piston number j, denoted ξ_j. Payout is defined positive when it adds elongation to the riser and negative in the opposite direction. *Minimum payout*, $\xi_{\min}$, means that the piston is as far into the cylinder as possible, for simplicity assumed zero here. *Maximum payout*, $\xi_{\max}$, refers to the position with maximum free piston length. The *initial payout*, ξ_0, is the distance between the lower end of the cylinder and the initial position. The total *dynamic payout* is given as

$$\xi_j(t) = \xi_0 + z_{init}(t) - z_{j,n+1}(t),\ j = 1,2. \tag{7}$$

where $z_{j,n+1}$ is the vertical top position of riser j. The dynamic payout with TLP motions is illustrated in Fig. 3.

Control Objectives

Today the top tension is kept close to constant by a passive heave compensation system for each riser. Keeping the tension

constant and equal in both risers may lead to the following scenario: For the two risers in tandem arrangement, R2 is in the wake of R1. Due to the shielding effects on R2, R1 will experience larger current and drag force than its downstream neighbor. If both risers have the same top tension, the deflection of R1 will exceed the deflection of R2, and the two risers may collide, shown in Fig. 5a). Another strategy is equal payout by connecting all risers to a common frame, proposed by Huse and Kleiven [7] and studied by Rustad *et al.* [8], see Fig. 5b). This will give varying top tension on the risers depending on the drag forces and the position in the riser array. Further studies addressed in this work have shown that due to this tension variation, two equal risers will experience different length due to axial strain according to

$$\Delta l_R = \frac{\Delta T}{EA} l_{R0}, \quad \Delta T = T_1 - T_2, \tag{8}$$

where Δl_R is the length variation due to the difference in top tension ΔT of the two risers. l_{R0} is the untensioned initial riser length, E is the modulus of elasticity and A is the cross sectional area. Collision can still occur, but less frequent and in a smaller riser segment than the equal tension strategy under the same environmental conditions. The risk of collision increase with increasing depth, in addition to the increasing effect of axial strains for longer riser lengths with larger tension variation.

In this work we propose a new control strategy letting the risers having equal effective length. By using automatic control of the heave compensators and top tension, the sum of payout and riser length should be equal such that the controller objective can be formulated as

$$\xi_1 + l_{R,1} = \xi_2 + l_{R,2}, \tag{9}$$

where $l_{R,j}$ is the length of riser j. This means that in contrast to the strategy of equal payout we also compensate for the axial elasticity due to the tension variation, see Fig. 5c). By introducing this way of controlling the top tension, the risers may be placed with closer spacing without increasing the risk of collision. Eq. (8) is a simplification valid for two equal risers. For risers with different characteristics with respect to diameter, riser material or filling a more general expression is needed. The riser length can be formulated as

$$l_{R,j} = l_{R,j}(T_{0,j}) + \Delta l_{R,j}, \quad \Delta l_{R,j} = \frac{T_j - T_{0,j}}{EA_j} l_{R0}, \tag{10}$$

where $l_{R,j}(T_{0,j})$ is the initial length of riser j with the initial tension T_{0j}. $\Delta l_{R,j}$ is the elongation of riser j relative to its initial

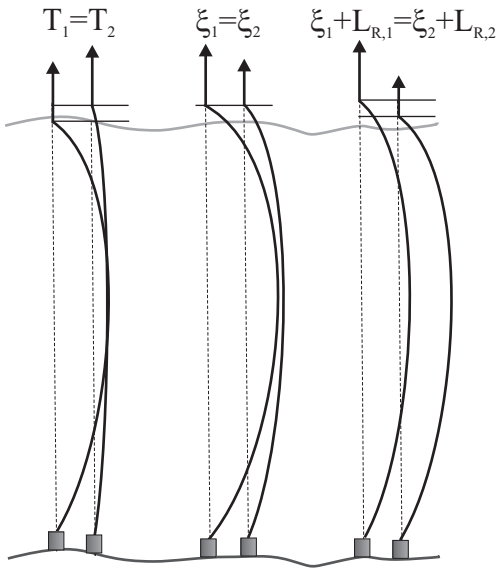

Figure 5. Effect of equal tension (a), equal payout (b), and equal effective length (c).

tension. Hence, Eq. (9) could be rewritten as

$$\xi_1 + l_{R,1}(T_{0,1}) + \Delta l_{R,1} = \xi_2 + l_{R,2}(T_{0,2}) + \Delta l_{R,2}. \tag{11}$$

The initial length and static payout can be found individually. However, note that the bottom of the cylinders need to be at the same level, for Eq. (11) to be valid, otherwise the difference needs to be compensated for. To summarize; the three different control objectives can be mathematically formulated as:

1. Equal tension: $T_1 = T_2$
2. Equal payout: $\xi_1 = \xi_2$
3. Equal effective length: $\xi_1 + l_{R,1} = \xi_2 + l_{R,2}$

Guidance and Reference Model

The guidance block is used to calculate the reference trajectory or set point for payout for each riser tensioner system. If one risers position is used as a reference trajectory for the other in the two-riser-system, the length variation as given in Eq. (10) is compensated for with

$$\xi_{r,2} = \xi_1 + l_{R,1}(T_{0,1}) + \Delta l_{R,1} - [l_{R,2}(T_{0,2}) + \Delta l_{R,2}], \tag{12}$$

where $\xi_{r,j}$ is the reference for the payout of riser j. If R2 is used as a reference, the indexes are switched.

To provide high performance in tension control between various control modes and/or setpoints, a reference model is introduced to calculate a feasible trajectory for the vertical position of

the top node decided in the guidance block. The following third order filter is demonstrated appropriate

$$\ddot{\xi}_d + 2\zeta_d \omega_d \dot{\xi}_d + \omega_d^2 \xi_d = \omega_d^2 \xi_{ref} \tag{13}$$

$$\dot{\xi}_{ref} = -\frac{1}{t_d}\xi_{ref} + \frac{1}{t_d}\xi_r, \tag{14}$$

where ξ_d and its derivatives are the desired payout position, velocity and acceleration trajectories. ξ_r is the new reference coordinates in the same frame, and ξ_{ref} is the low pass filtered coordinate. ζ_d is the relative damping ratio, ω_d is natural frequency, and t_d is the cut-off period period of the low pass filter in Eq. (14). This provides a smooth transfer between different setpoints.

Plant Controller

A PI-controller for each riser is introduced to adjust the top tension according to the reference trajectory and the actual position of the individual riser

$$\tau_{c,j} = -K_{P,j} e_j - K_{I,j} \int e_j dt \tag{15}$$

$$e_j = \xi_{d,j} - \xi_j \quad j = 1,2, \tag{16}$$

where $K_{P,j}$ and $K_{I,j}$ are the positive control gains for riser j. The top tension in each riser is then the pretension, $T_{0,j}$, plus the contribution from the controller $\tau_{c,j}$

$$T_j = T_{0,j} + \tau_{c,j} \quad j = 1,2. \tag{17}$$

An appropriate integrator wind-up algorithm must also be implemented avoiding undesired integrator discharge.

SIMULATIONS

The riser model was verified with a variety of current profiles. However, the simulations included in this paper are all from the Ormen Lange field. In addition to current field found in Fig. 2, a variance in the in the current is made by filtering with noise through a low pass filter with a period of 100s, and an amplitude within the band of 5% of the current velocity in each node. Most simulations are executed about zero and 30m static offset. The center-to-center distance is 15D at 1200m water depth.

Control Strategies

All three different control objectives are tested and compared. The equal payout and equal effective length control objectives are exemplified by control of R2 using the payout of R1 as the reference.

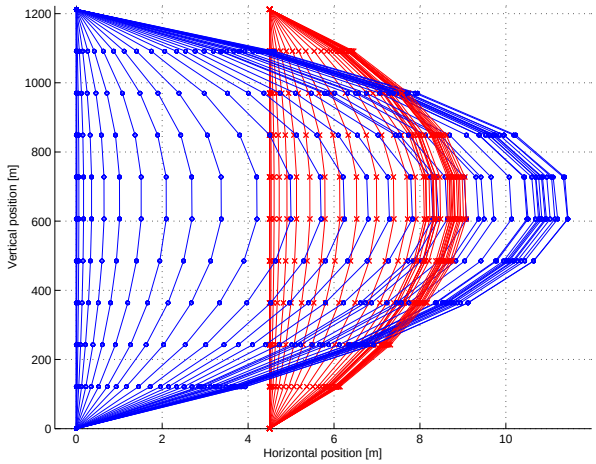

Figure 6. Snapshot of the riser configuration, for incrementing current velocity from zero to the Ormen Lange design current.

Constant Equal Tension In the first case, the top tension of the risers are equal and constant. The incoming current profile is increased as a second order lowpass filtered step from zero to the design current profile. A medium top tension of $T_{o,i} = 1800$kN is applied, and there is no TLP offset. As the current increases, the risers are seen to slide out to the right in Fig. 6. The maximum horizontal deflection is seen at 600m above the seabed. Collision occurs along almost the entire riser, seen in nodes 3 to 9.

The TLP is then put in an offset position of 30m, with increasing current, seen in Fig. 7. The TLP is not very likely to have an offset in the opposite direction of the surface current, so the offsets are only simulated in the positive direction. Collision is seen to occur in the same nodes independent of the offset position. The horizontal positions for three selected nodes are shown in Fig. 8a), where it is seen that collision occurs at the first node after approximately 400s. The corresponding payout due to deflection is seen in Fig. 8b). R1 has largest deflection and hence setdown, which is clearly seen in the payout plot.

Increasing the top tension to the upper limit of $T_{0,i} = 2700kN$, collision does not occur in any nodes in any of the simulated current profiles (not shown here). Keeping the tension at the upper limit, collision could be avoided for these design currents. However, to operate the risers at this tension level is not desired due to increased stress in the riser and excessive wear of the tension system. For the rest of the simulations, the pretension is kept to $T_{0,i} = 1800kN$ for both risers. A fully developed current profile for the Ormen Lange field is used.

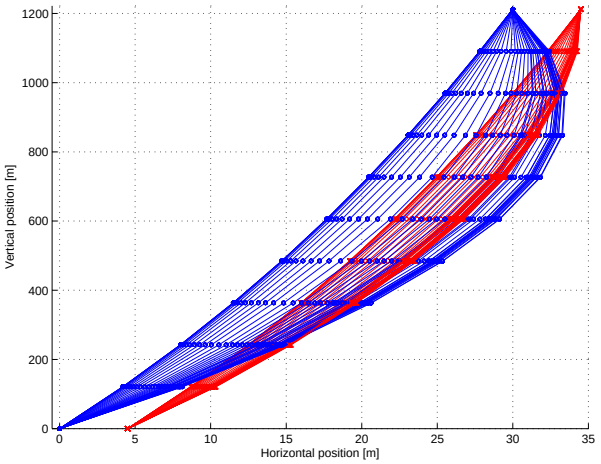

Figure 7. Incremental current at Ormen Lange with 30m offset.

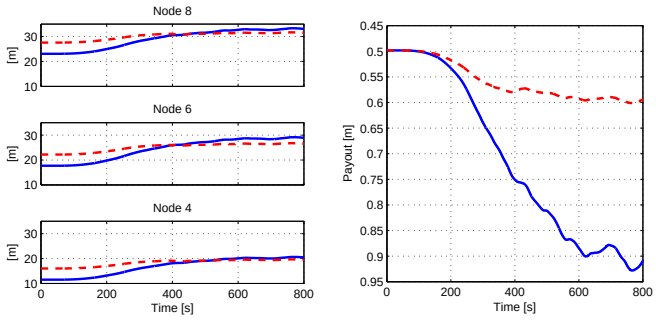

Figure 8. From left: a) Horizontal position of three nodes. b) Payout. Both for increasing current velocity and 30m offset, R1 (–), R2(- -).

Equal Payout For the equal payout controller strategy, the payout of R1 is used as reference for R2

$$\xi_{r,2} = \xi_1. \tag{18}$$

This control algorithm gives equal payout for the risers, seen in Fig. 9b). Fig. 9a) shows how R2 slides out to the right due to decreased tension. However, collision does still occur, but in a smaller riser segment than with equal tension (nodes 5-6). This is caused by the lower tension in R2 compared to R1, which in turn gives less axial elongation, and a shorter R2 than R1. Hence, due to the elasticity of steel, collision may still occur using equal payout.

Equal Effective Length The elasticity of steel needs to be included in the guidance trajectory which for equal risers are

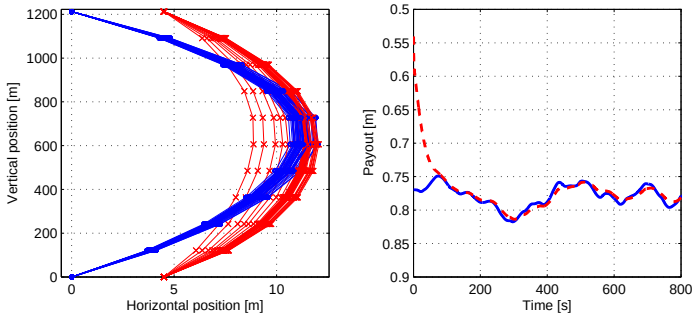

Figure 9. Equal payout algorithm and control of R2. From left: a) Snapshots. b) Corresponding payout for R1(–) and R2(- -).

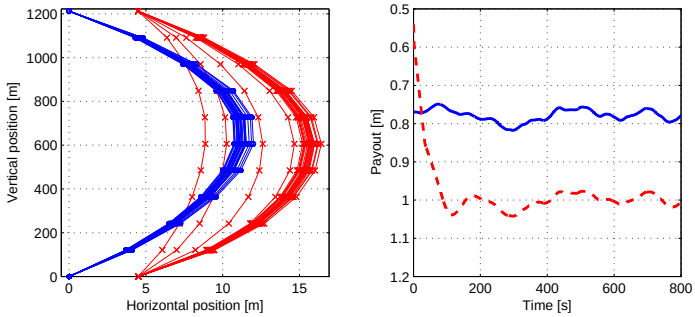

Figure 10. Equal effective length and control of R2. From left: a) Snapshots. b) Corresponding payout for R1(–) and R2(- -).

simplified to

$$\xi_{r,2} = \xi_1 + \Delta l_R. \tag{19}$$

The snapshots in Fig. 10a) show how the mid-position of R2 starts in front of R1 when the pretensions are equal. R2 then slides out to the right to avoid collision as the tension decreases, and the payout of R2 approaches the reference trajectory and both risers achieve similar deflection. The smaller variation in the horizontal position is due to variance in the current. In Fig. 10b) we clearly see that R2 has a larger payout to compensate for lower tension, and to achieve equal effective length.

The same algorithm is conducted for 30m TLP offset (Fig. 11). As before R2 slides out to the right with decreasing tension, increasing the horizontal distance between the risers to avoid collision, see Fig. 11a). The payout, seen in Fig. 11b) is larger in the offset case than without offset due to the effects from weight and current. For top tension, T_2, stabilize about 1400kN for the offset case and 1300kN for the non-offset case, not shown here. Hence, a smaller tension difference is needed in the offset position. This is due to a longer effective length of the riser and payout, and the

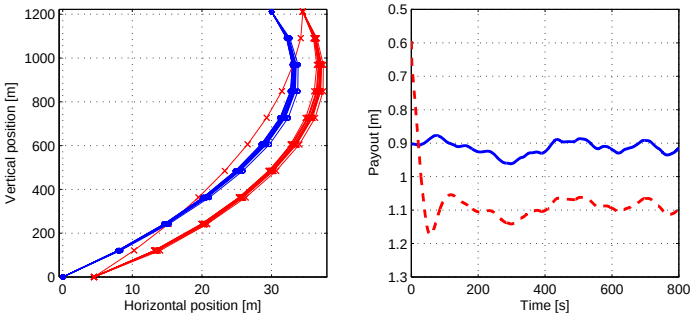

Figure 11. From left: a) Snapshots with 30m offset, equal effective length and control of R2. b) Payout for R1(–) and R2(- -)

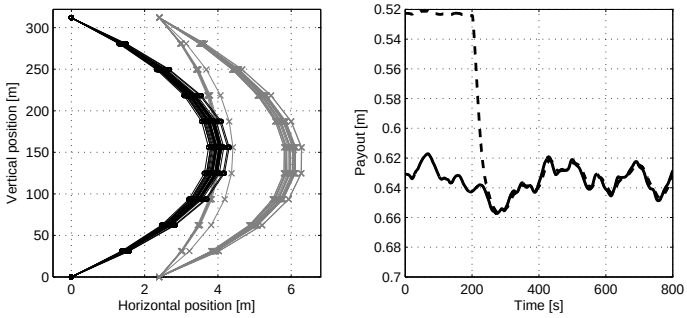

Figure 12. From left: a) Snapshots of equal payout control of R2 at 300m water depth. b) Corresponding payout for R1(–) and R2 (- -).

relation between tension, payout and horizontal deflection. For a long riser with small tension, an increase in tension has larger effect on the lateral deflection, than if the riser already has a high tension level.

Effect of Shallow Water

The effect of the two active control objectives in shallow water is then investigated. The risers are placed at 300m and the current profile from the Ormen Lange field is scaled to this new water depth, keeping the same velocity in each node. The risers have the same physical dimensions as before, except for the length. The center-to-center distance is decreased to 8D. Keeping the same riser diameter, the upper tension limit could be the same due to stress considerations, whereas the lower tension limit is due to effective weight. Here, the water depth and also the effective weight is one forth of the previously simulated depth of 1200m. The lower tension limit could be as low as 350kN at 300m water depth. The tension level is much lower and the axial elongation therefore smaller, according to $\Delta l = \frac{T}{EA} l_0$, and hence excepted to be of less importance. The equal payout and the equal effective length control objectives are tested with an initial tension of 600kN, zero offset and control of R2, starting after 200s. Fig. 12a) shows how R2 slides out to the right due to the decreased tension when the control is turned on. The payout is seen to be equal for the two risers in Fig. 12b). For the equal effective length in Fig. 13, R2 slide slightly more to the right, and the payout is seen to be 2-3cm larger for R2 than for R1, due to the elasticity compensation. The tension of R2 is right above 400kN using equal payout and right below 400kN using the equal effective length control objective, not shown here. The relative horizontal distance between the risers is about 7D in the first case and 8D in the latter. A small effect of taking the elasticity into account is seen even at 300m water depth. However, it is of far less importance than at deeper waters.

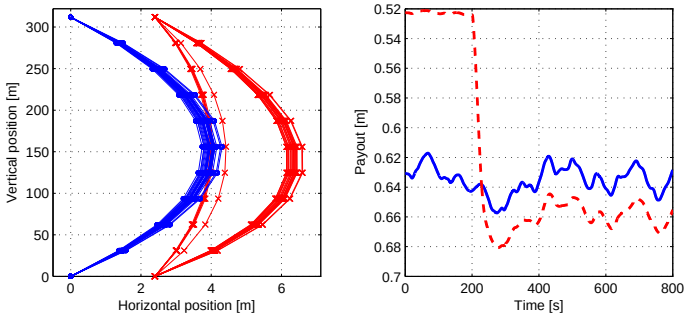

Figure 13. From left: a) Snapshots of equal effective length control of R2 at 300m water depth. b) Corresponding payout for R1(–) and R2 (- -).

TLP Dynamics

For the last simulation 1200m water depth is used. In this case the TLP moves with harmonic motions in surge direction about a static offset of 30m. The period is 120s, and the peak-to-peak amplitude 40m. The controllers are enabled after 400s. Fig. 14a) shows the horizontal positions for three selected nodes. In the case where R2 is controlled, we see that the collision is avoided by increasing the horizontal position of R2. The riser slides out to the right when the payout increases. It is seen in these plots, as expected, that the upper nodes are most influenced by the TLP motion. When R1 was controlled, the horizontal positions of R1 decreased, and the horizontal positions for R2 increased at the same time due to reduced shielding, not shown here.

Fig. 14b) shows the relative horizontal position between the same three nodes. The effect of control is clearly seen. Before the controller is turned on, collision occurs twice for each cycle. After 400s, the controller is turned on, and the mean distance is about 15D, equal to the top and bottom distance, for all nodes, giving a similar configuration for the two risers. Also, the variation in distance between corresponding nodes decreases

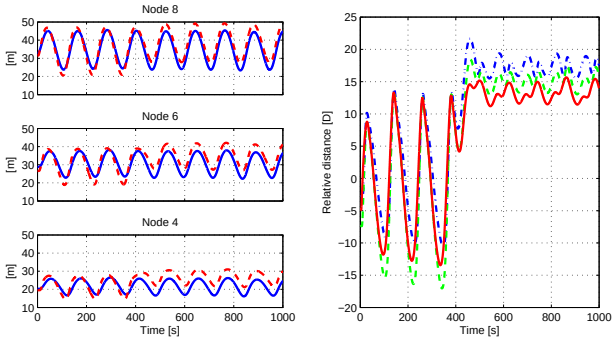

Figure 14. From left: a) Horizontal positions of nodes with dynamic TLP motions without and with control of R2 enabled after 400s. R1(–), R2(- -). b) Corresponding relative horizontal position of nodes 4(-.), 6(- -) and 8 (–).

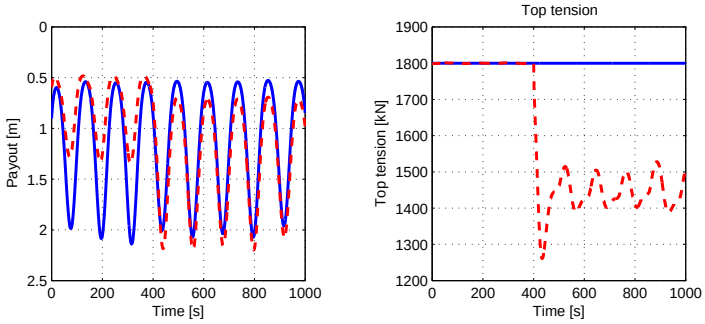

Figure 15. From left: a) Payout with dynamic TLP motion without and with control of R2 enabled after 400s. b) Corresponding top tension of R1(–) and R2(- -).

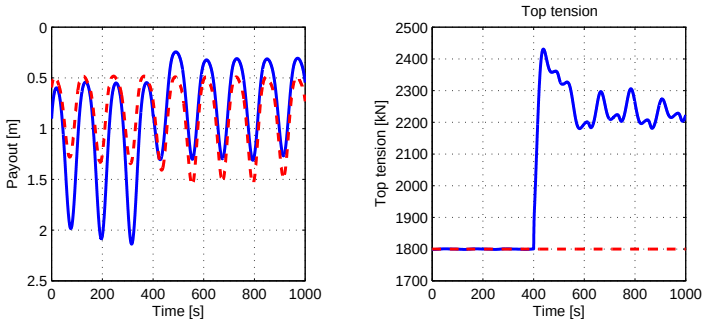

Figure 16. From left: a) Payout with dynamic TLP motion without and with control of R1 enabled after 400s. b) Corresponding top tension of R1(–) and R2(- -).

significantly. The payout with control of R1 and R2 are given in Figs. 15a) and 16a), respectively. For the uncontrolled case, the dynamic stroke of R1 is 1.6m and for R2 0.8m. This is due to drag and deflection on R1 due to dynamically TLP motion giving larger demand for stroke. R2 has a more straightlined configuration due to reduced current and drag. Also, it should be noted that when R2 comes in front, the model is not valid, and R2 keeps its straight configuration.

However, when R1 is the reference, the stroke of R2 is increased, and the stroke of R1 is slightly decreased, giving a dynamic stroke about 1.5m for both risers. The mean tension of R2 is decreased to about 1450kN, giving a tension difference of 350kN between the risers, see Fig. 15b). The smaller mean tension compared to the static case is due to longer payout and total effective length, such that a smaller tension difference is needed to avoid collision. The dynamic tension variation has a period of 120s as for the TLP, and a peak-to-peak amplitude about 120-140kN.

When R2 is the reference for R1, its dynamic stroke decreases, giving both R1 and R2 a dynamic stroke about 1m, see Fig. 16a). The mean tension level increased with 400kN for T_1, seen in Fig. 16b). The dynamic tension variation was about 120-130kN. Increasing the TLP period to 300s, a more quasi-static riser behavior is seen with less dynamic deflection. This gives less need for stroke, a smaller payout and effective length and a larger tension difference, closer to the static case.

Riser Properties

The risers in an array do often not have the same physical properties. The external diameter, wall thickness, and density of the internal fluid could vary, depending on whether the the riser is used for drilling, production, export or workover. Together these factors decide the dynamics of the riser. Different cross sectional area gives different elongation proportional to the elasticity; EA. The cross sectional area also contributes to a weight difference, increased or decreased by the difference in the density of the internal fluid between the risers. The effective weight decides the tension level, which in turn gives the eigenperiods of the risers. The effective weight gradient also affect the dynamics. In extreme cases the longest riser eigenperiod can be close to the the typical low frequency motions. For another riser case, the first eigenperiod could be close to the slowest wave frequency motions. In addition it should be noted that the current field behind a riser and the shielding effect, is dependent on the diameter of the upstream riser. The effects of the riser properties should be taken into consideration when deciding the control strategy.

CONCLUDING REMARKS

Three different control objectives and strategies are presented and their respective range of application are investigated. A simulation study of the two risers in tandem attached to a TLP

has been carried out. For very low current velocities, equal tension can be sufficient. Equal payout is shown appropriate at shallow water. However, at deeper water the effect of elasticity and riser elongation needs to be included in the control strategy in order to avoid riser collision.

ACKNOWLEDGMENT

The work has been carried out at Centre for Ships and Ocean Structures (CeSOS), NTNU. The Research Council of Norway is acknowledged as the main sponsor of CeSOS.

REFERENCES

[1] Huse, E., 1993. "Interaction in Deep-Sea Riser Arrays". In Proc. of the 25th Annual Offshore Technology Conference, pp. 313–322. OTC7237.

[2] Wu, W., Huang, S., and Barltrop, N., 2001. "Multiple Stable/Unstable Equilibria of a Cylinder in the Wake of an Upstream Cylinder". In 20th Int. Conf. on Offshore Mech. and Arctic Eng. OMAE2001/OFT-1170.

[3] Herfjord, K., Holmås, T., Leira, B., Brydum, M., and Hanson, T., 2002. "Computation of Interaction between Deepwater Risers, Collisionstatistics and Stress Analysis". In 21th Int. Conf. on Offshore Mech. and Arctic Eng. OMAE2002-28152.

[4] Kalleklev, A. J., Mørk, K. J., Sødahl, N., Nygård, M. K., and Horn, A. M., 2003. "Design Guidelines for Riser Collision". In Proc. of the Annual Offshore Technology Conference. OTC15383.

[5] Huse, E., 1996. "Experimental Investigation of Deep Sea Riser Interaction". In Proc. of the 28th Annual Offshore Technology Conference, pp. 367–372. OTC8070.

[6] DNV, 2005. Recommended practice for riser interference. Industry version issued DNV-RP-F203, Det Norske Veritas.

[7] Huse, E., and Kleiven, G., 2000. "Impulse and energy in deepsea riser collisions owing to wake interference". In Proc. of the Annual Offshore Technology Conference, OTC, p. OTC11993.

[8] Rustad, A. M., Larsen, C. M., Triantafyllou, M. S., Hover, F. S., Jacobsen, A. H., and Sørensen, A. J., 2006. "Modelling and control of colliding top tensioned risers in deep waters". In the 7th IFAC Conf. on Manoeuvering and Control of Marine Crafts.

[9] Rustad, A. M., Larsen, C. M., and Sørensen, A. J., 2007. "FEM Modelling and Control for Collision Prevention of Top Tensioned Risers". *J. of Marine Structures*(Accepted to appear).

[10] Kavanagh, W. K., Imas, L., Thompson, H., and Lee, L., 2000. "Genesis Spar Risers: Interference Assessment and VIV Model Testing". In Proc. of the Annual Offshore Technology Conference. OTC11992.

[11] Aker Maritime, 2002. Ormen Lange TLP with full processing facilities. Tech. Rep. 37-00-NN-X15-00117.

[12] Nowlin, W. D., Jochens, A. E., DiMarco, S. T., Reid, R. O., and Howard, M. K., 2001. Deepwater physical oceanography reanalysis ans synthesis of historical data. Synthesis Report MMS 2001-064, Dept. of Oceanography, Texas A & M Univeristy, New Orleans, USA.

[13] Jeans, G., Grant, C., and Feld, G., 2003. "Improved current profile criteria for deepwater riser design". *J. Offshore Mechanics and Arctic Engineering,* **125**, November, pp. 221–224.

[14] Fylling, I., Larsen, C., Sødahl, N., Omberg, H., Engseth, A., Passano, E., and Holthe, K., 2005. Theory Manual RiflexTM-34-rev0, SINTEF Marintek, Trondheim, Norway.

[15] Sørensen, A. J., 2005. "Structural Issues in the Design and Operations of Marine Control Systems". *Annual Reviews in Control,* **29**, pp. 125–149.

[16] Larsen, C., 1993. Analysis of tensioner system stroke for marine risers. Tech. Rep. STF70 F93011, SINTEF Structures and Concrete, January.

Appendix A: Simulation Parameters

α_2	Damping coefficient	0.047	-
D	Diameter	0.3	[m]
t_h	Wall thickness	0.015	[m]
C_D	Drag coefficient	1.0	-
E	Modulus of elasticity	206	[GPa]
f_u	Yield stress steel	500	[MPa]
ρ_s	Specific weight for steel	7850	[kg/m^3]
ρ_f	Specific weight for filling	800	[kg/m^3]
ρ	Specific weight for water	1026	[kg/m^3]
K_P	Proportional gain 300/1200m	1e6/607500	-
T_I	Integration time 300/1200m	8.5/8	[s]